ROYAL SOCIETY OF CHEMISTRY

REVIEW

Check for updates

Self-targeting of zwitterion-based platforms for nano-antimicrobials and nanocarriers

Da-Yuan Wang,†[ab] Linzhu Su,†[ab] Guang Yang,[ab] Yijin Ren,[c] Mingqing Zhang,[de] Haoren Jing,[e] Xipeng Zhang,[e] Roger Bayston, [ID][f] Henny C. van der Mei,*[b] Henk J. Busscher*[b] and Linqi Shi [ID] *[a]

Self-targeting antimicrobial platforms have yielded new possibilities for the treatment of infectious biofilms. Self-targeting involves stealth transport through the blood circulation towards an infectious biofilm, where the antimicrobial platform penetrates and accumulates in a biofilm in response to a change in environmental conditions, such as local pH. In a final step, nano-antimicrobials need to be activated or the antimicrobial cargo of nanocarriers released. Zwitterions possess both cationic and anionic groups, allowing full reversal in zeta potential from below to above zero in response to a change in environmental conditions. Electrolyte-based platforms generally do not have the ability to change their zeta potentials from below to above zero. Zwitterions for use in self-targeting platforms are usually hydrophilic and have a negative charge under physiological conditions (pH 7.4) providing low adsorption of proteins and assisting blood circulation. However, near or in the acidic environment of a biofilm, they become positively-charged yielding targeting, penetration and accumulation in the biofilm through electrostatic double-layer attraction to negatively-charged bacteria. Response-times to pH changes vary, depending on the way the zwitterion or electrolyte is built in a platform. Self-targeting zwitterion-based platforms with a short response-time *in vitro* yield different accumulation kinetics in abdominal biofilms in living mice than platforms with a longer response-time. *In vivo* experiments in mice also proved that self-targeting, pH-responsive zwitterion-based platforms provide a feasible approach for clinical control of bacterial infections. Clinically however, also other conditions than infection may yield an acidic environment. Therefore, it remains to be seen whether pH is a sufficiently unique recognition sign to direct self-targeting platforms to an infectious biofilm or whether (additional) external targeting through *e.g.* near-infrared irradiation or magnetic field application is needed.

1. Introduction

The increase in the number of antimicrobial-resistant bacterial strains makes clinical treatment of infection more and more difficult. Causative to the problems associated with infection treatment are the intrinsic antimicrobial-resistance of many strains and the recalcitrance to antimicrobial penetration of

[a] *State Key Laboratory of Medicinal Chemical Biology, Key Laboratory of Functional Polymer Materials, Ministry of Education, Institute of Polymer Chemistry, College of Chemistry, Nankai University, Tianjin 300350, P. R. China. E-mail: shilinqi@nankai.edu.cn*

[b] *University of Groningen and University Medical Center Groningen, Department of Biomedical Engineering, Antonius Deusinglaan 1, Groningen 9713 AV, The Netherlands. E-mail: h.c.van.der.mei@umcg.nl, h.j.busscher@umcg.nl*

[c] *University of Groningen and University Medical Center Groningen, Department of Orthodontics, Hanzeplein 1, Groningen 9700 RB, The Netherlands*

[d] *Nankai University School of Medicine, Nankai University, Tianjin, China*

[e] *Department of Colorectal Surgery, Tianjin Union Medical Center, Tianjin, China*

[f] *University of Nottingham, School of Medicine, Nottingham, UK*

† These authors contributed equally to this work.

infectious biofilms. Antimicrobial penetration and subsequent accumulation in a biofilm are hampered by slow diffusion of antimicrobials into a biofilm, including adsorption to the walls of water-filled channels in a biofilm.[1] Accordingly, bacteria residing in the surface region of an infectious biofilm are exposed to the highest antimicrobial concentration, while bacteria residing in deeper regions of a biofilm often escape killing by antimicrobials.[2]

Antimicrobial diffusion into a biofilm is critically controlled by the concentration at which the antimicrobials are applied. However, many antibiotics cause severe side-effects when applied at too high concentrations. Such side-effects are currently avoided by application of high, local antibiotic concentrations around an infection site. Highly porous, gentamicin-loaded acrylic bone cement beads have been implanted in osteomyelitis patients to generate high local antibiotic concentrations around infected bone.[3] Also, primary joint arthroplasties are fixated in bone using antibiotic-loaded cements in order to prevent infection. Central venous catheter-associated bacteraemia can be prevented by the

use of an antibiotic lock or cuff around the catheter creating a high antibiotic concentration at the point of bacterial entry in the body.[4]

Though effective, local antimicrobial delivery devices have drawbacks. Gentamicin-loaded acrylic beads used in the treatment of osteomyelitis not only require surgical implantation, but also removal. Release kinetics from delivery devices often include a burst-release, followed by a low-level tail-release that can extend up to several years with the risk of inducing antibiotic-resistance.[5] Most importantly, burst-release occurs regardless of whether or not an infection actually exists, implying the low-level tail-release may be insufficient to yield bacterial killing at the time of need.

Nano-antimicrobials and antimicrobial-loaded nanocarriers currently under design provide an array of new possibilities to generate high local concentrations of antimicrobials around an infection site.[6] Nano-antimicrobials and antimicrobial-loaded nanocarriers can be directed to an infectious biofilm using external triggers, such as an applied magnetic field or light irradiation. Directing can also be done in response to environmental changes around an infection site as compared with healthy, physiological conditions ("self-targeting"). Self-targeting (see Fig. 1) implies that an antimicrobial can be injected anywhere in the blood circulation, and can subsequently travel undisturbed, in a "stealth" way through the blood flow from where it recognizes an infectious biofilm.[7] Recognition of a biofilm can be done based on a change in environmental conditions, that may include local pH,[8] hypoxia,[9] macrophage presence and increased ROS levels,[10] specific ligand-receptor binding[11] or increased local temperatures.[12] Environmental recognition signals mostly induce a change in the properties of an antimicrobial from hydrophilic ("stealth")

towards more hydrophobic and becoming more positively charged. Due to a more positive charge, electrostatic double-layer attraction with negatively-charged bacterial cell surfaces[13] will reduce electrostatic double-layer repulsion or even cause electrostatic double-layer attraction. This depends on whether the charge has remained negative under the conditions of the environmental change or has been fully reverted from below to above zero. Accordingly, the combination of altered electrostatic double-layer forces and ubiquitously present, attractive Lifshitz-van der Waals forces yields a net attraction to cause penetration in a biofilm and prevent subsequent washout. After self-targeting, an antimicrobial needs to be activated or released from its carrier as a final step towards killing bacterial inhabitants in an infectious biofilm. The above described, sequential steps in self-targeting are summarized in Fig. 1. Self-targeting has been found to greatly enhance the killing of bacterial pathogens housed in a protective, infectious biofilm by antimicrobials.[7,14]

Self-targeting nano-antimicrobials or nanocarriers can be based on zwitterionic or electrolyte platforms. Zwitterionic molecules distinguish themselves from electrolytes by the possession of an identical number of both cationic and anionic groups and in ionic form present themselves as positively or negatively charged depending on environmental conditions. Electrolytes possess either cationic or anionic groups and present themselves as a neutral molecule, or in an ionic form, as carrying a positive or negative charge. Typical cationic molecules involve amino groups, quaternary amine salts and protonated water, while anionic groups on zwitterionic molecules include carboxylate and sulfonate groups (see Fig. 1). Since infectious biofilms in the human body are more acidic than their healthy, physiological environment,[15] responsiveness to local pH makes zwitterion-based platforms ideally suitable for use as self-targeting moieties in smart nano-antimicrobials and nano-carriers (see also Fig. 1).

In this review, we will first summarize different types of zwitterions and their responsiveness in different platforms to pH changes, as compared with electrolytes. Possible clinical merits of self-targeting zwitterion-based nano-antimicrobials and nanocarriers will be evaluated in view of their responsiveness to pH changes. Therewith, we hope to focus future research into self-targeting nano-antimicrobials or antimicrobial nanocarriers for bacterial infection control towards clinical translation.

Fig. 1 Summary of different anionic and cationic groups occurring in zwitterions, and the pH responsive groups required for self-targeting. The different steps in self-targeting are outlined in the outer circle of the diagram, numbered in the order of occurrence during self-targeting.

2. pH responsive zwitterions

In this section, we will describe different types of zwitterionic molecules that are being used in self-targeting nano-antimicrobials and nanocarriers responding to different pH conditions. In Table 1, the structure formulas of different zwitterionic molecules are summarized with their iso-electric points. As can be seen, iso-electric points vary widely to well above pH 5.0, generally assumed to be the pH in infectious biofilms,[14] to well below pH 5.0. Zwitterionic DOAAQ-, sulfo-betaine- and phosphobetaine-based platforms have an

Table 1 Zwitterions used in different pH-responsive nano-antimicrobials or antimicrobial nanocarriers together with their structure formulas and iso-electric points. Zwitterionic molecules are indicated by their abbreviations, as defined in the references given

Abbreviation	Structure formula	Iso-electric point	Ref.
DCPA–H_2O		6.8–7.0	8
ZTC		6.5–6.8	17
PGlu(DET-Car)		6.5	19
DOMPAQ		6.4	20
PQAE		6.2	17
G3′-SB		5.5	21
DOMPAT		5.5	20
Carboxybetaine		4.7	22
DOAAQ		3.6	20
Sulfobetaines		2.8	22
Phosphobetaines		2.1	22

extremely low IEP, implying that they remain negatively charged under acidic conditions occurring in an infectious biofilm. This makes these platforms unsuitable for use as smart nano-antimicrobials or antimicrobial nanocarriers. The advantage of using zwitterions above electrolytes as a pH-responsive molecule in self-targeting nano-antimicrobials and nanocarriers, follows from a comparison of their zeta potential change under physiological pH and under the pH in an acidic biofilm. The zeta potential of electrolyte-based self-targeting nano-antimicrobials and nanocarriers is either negative or positive regardless of pH and although becoming more positive under acidic conditions, electrolytes seldom display a change in zeta potential from below to above zero at lower pH (Fig. 2a). PAE is an exception in the sense that it displays a small change in zeta potential from just below to just above zero when pH changes from 7.4 to 5.0. Zwitterion-based platforms on the other hand, yield a full charge reversal from below to above zero (Fig. 2b), which may be considered an advantage in self-targeting platforms.

Response times for effectuating charge changes upon a change in environmental pH differ greatly across different electrolyte- and zwitterion-based platforms, although response times are not consistently reported in the literature. Electrolyte-based platforms can respond relatively fast, such as the PAE-based micelles presented in Fig. 2a, reported to be less than 5 min.[16] PEG-PDLLA electrolyte-based micelles on the other hand, require up to 24 h to establish a full charge change upon exposure to an acidic environment (Fig. 2c). Likely, these differences are due to

way the molecule is incorporated in the micellar shell. For the same reason, zwitterion-based platforms also have highly different response times. Zeta potentials of PQAE micelles changed within 2 h after changing pH conditions from 7.4 to 5.0 (see Fig. 2d), due to condensation of hydroxyl groups attached to nitrogen forming a lactone ring, as confirmed by a time-dependent chemical shift in ^{1}H NMR spectrum at the α-position of the hydroxyl.[17] Zwitterion-based ZTC-NM nanoparticles responded to a pH decrease with an approximately similar response time of 3 h.[18] This may lead to the careful conclusion, that zwitterion-based platforms may respond faster to a change in pH than electrolyte-based platforms.

3. Self-targeting of infectious sites

Penetration and accumulation constitute an important step in self-targeting and are mostly demonstrated *in vitro* by growing a biofilm in a well plate and exposing the biofilm to a self-targeting platform under physiological pH and under a more acidic pH.[2,26] Typically, penetration and accumulation are visualized using fluorescently labelled platforms (see Fig. 3). However, under the static fluid conditions in a well plate, response to a different pH occurs due to the pH in the well itself. This not only implies the presence of a biofilm with a local, acidic pH inside, but in fact the entire biofilm is completely surrounded by a pH 5.0 environment. Therefore, these frequently carried out experiments to demonstrate self-targeting,[17,27] do not encompass a true recognition sign that directs a self-targeting platform to an infectious biofilm. Thus, well plate experiments only yield proof-of-principle of enhanced penetration and accumulation, but not of self-targeting as a whole.

Arguably, experiments to demonstrate self-targeting of nano-antimicrobials or antimicrobial nanocarriers can only be adequately done *in vivo*. Real-time observation of the arrival of fluorescent nano-antimicrobials or nanocarriers from the blood circulation at an infection site can be made in living mice, with an implanted abdominal window.[28] In a typical experiment, a fluorescent self-targeting platform is tail-vein injected in a living mouse (see schematic in Fig. 4a), after which it has to self-target through the blood circulation till the platform encounters an infectious biofilm, growing underneath an abdominal window surgically implanted in the flank of the mouse (Fig. 4b). The window subsequently allows direct microscopic observation of the arrival of a fluorescently labeled platform in the abdominal biofilm. In Fig. 4c arrival times of different, fluorescently labeled platforms in an abdominal staphylococcal biofilm after tail-vein injection are compared. DCPM and DPPC lipid liposomes do not recognize a biofilm while circulating in the blood and accordingly demonstrate no accumulation in the biofilm after tail-vein injection. The zwitterion-based PQAE and DCPA–H_2O platforms self-target through recognition by electrostatic double-layer attraction and accumulate in the abdominal biofilm. PQAE micelles have a response time with respect to pH decrease and zeta potential of around 120 min and show a somewhat delayed, gradual accumulation in the biofilm. The response times of DCPA–H_2O with respect to pH decrease and zeta potential are not available

Fig. 2   Zeta potentials at pH 5.0 and pH 7.4 and response times to pH changes of different electrolyte- and zwitterion-based platforms used in nano-antimicrobials and nanocarriers. (a) Zeta potentials of different electrolyte-based platforms. DCPM, PEO-*b*-PAA, DOTAP and PAE indicate electrolyte-based platforms composed of ((4-((1,5-bis(octadecyloxy)-1,5-dioxopentan-2-yl) carbamoyl)-1-methylpyridin-1-ium)),[8] poly(ethylene oxide)-*block*-poly(acrylic acid)[23] 1,2-dioleoyl-3-trimethylammonium-propane,[24] and (β-amine ester),[16] respectively. (b) Zeta potentials of different zwitterion-based platforms. For abbreviations, structure formulas and references see Table 1. (c) Zeta potentials of electrolyte-based PEG-PDLLA micelles as a function of time upon a change in pH from 7.4 to 5.0. Data are taken from Sun *et al.*[25] and reproduced with permission from Wiley (d) Zeta potentials of zwitterion-based PQAE micelles as a function of time upon a change in pH from 7.4 to 5.0. Data are taken from Tian *et al.*[17] and reproduced with permission from American Association for the Advancement of Science.
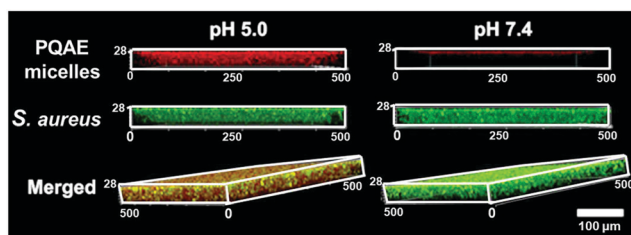

Fig. 3   Confocal laser scanning micrographs of Nile-red loaded, zwitterionic PQAE micelles accumulated into green fluorescent, 48 h-old *Staphylococcus aureus* biofilms after 30 min of penetration from phosphate buffered saline at pH 5.0 and 7.4. Micrographs taken from Tian *et al.*[17] and reprinted with permission from the American Association for the Advancement of Science.

but can be assumed to be around 8 min, based on ^{1}H NMR chemical shifts in DCPA–H$_2$O spectra exposed to different pH environments.[7] Interestingly, this relatively short response time is accompanied by an immediate, gradual increase in accumulation. Self-targeting zwitterion-based platforms with a short response time thus yield a different accumulation kinetics in an infectious biofilm than platforms with a longer response time.

Arguably, also experiments to demonstrate blood compatibility of self-targeting platforms can only be done *in vivo*. *In vitro* experiments have shown that particularly zwitterion-based platforms adsorb very little protein.[19,29] However, often these *in vitro* experiments are done either with selected proteins,[30,31] diluted plasma,[8,32] or in absence of flow.[33,34] Accordingly, the *in vivo* experiments outlined in Fig. 4 not only serve to illustrate self-targeting *in vivo*, but also provide stronger and more affirmative proof of blood compatibility than can be obtained *in vitro*. Good blood compatibility enables prolonged circulation in the blood which increases the chance of a self-targeting platform to meet its target, generally leading to a significant enhancement in targeting efficiency.[35,36]

4. Clinical merits of self-targeting *versus* targeting platforms for nano-antimicrobials and antimicrobial nanocarriers

From the above mini-review, it can be concluded that all requirements set to a self-targeting platform for nano-antimicrobials or
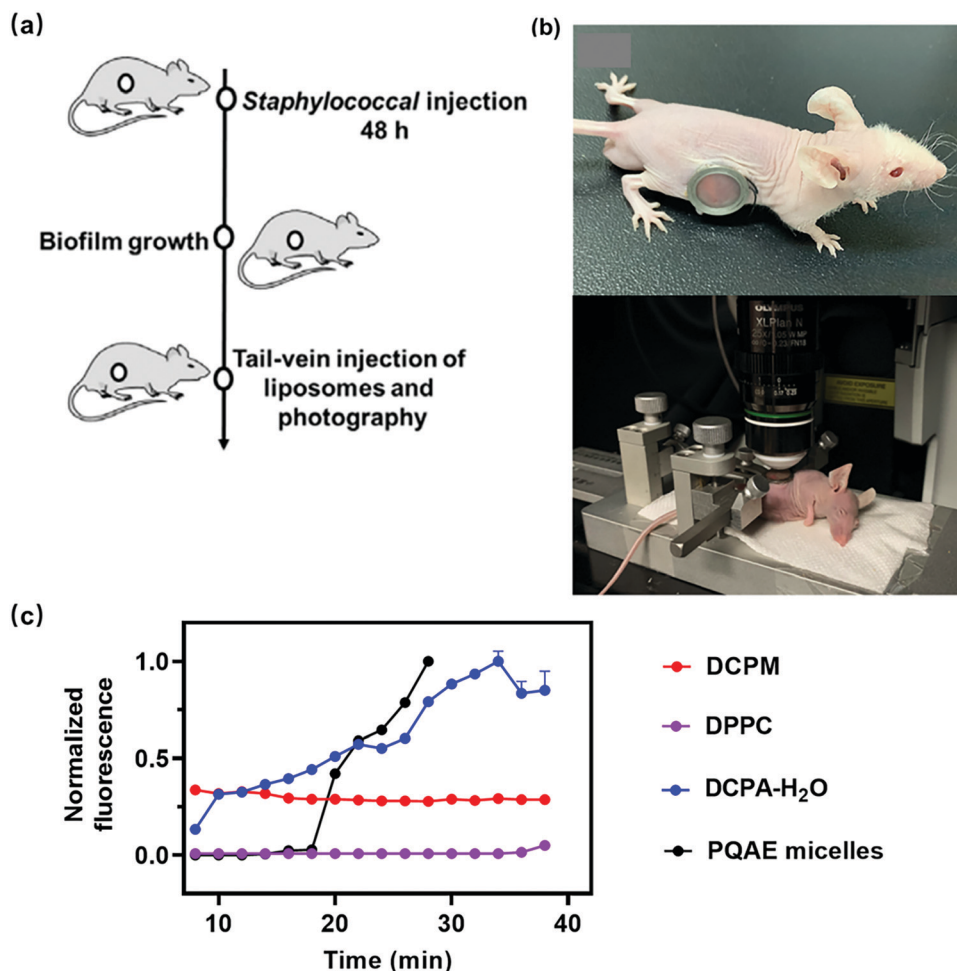
Fig. 4 (a) Schematic of the experimental sequence to study self-targeting of tail-vein injected fluorescent nanocarriers to an abdominal biofilm in living mice. (b) A mouse with an abdominal imaging window implanted in its flank underneath which a green-fluorescent *S. aureus* biofilm is grown (top photograph). The mouse can be fixed on a custom-designed microscope stage by clamping the window frame in a holder to ensure proper intravital focusing over time (bottom photograph).[8,17] Reprinted with permission from American Association for the Advancement of Science and Wiley. (c) Red-fluorescence intensity due to arrival of Nile-red loaded platforms in an abdominal biofilm as a function of time after tail-vein injection, expressed as a normalized red-fluorescent intensity with respect to maximal red-fluorescent intensity observed after 30 min. Abbreviations and references for zwitterion-based PQAE micelles and (DCPA−H$_2$O) liposomes can be found in Table 1. DCPM and DPPC indicate liposomes composed of ((4-((1,5-bis(octadecyloxy)-1,5-dioxopentan-2-yl) carbamoyl)-1-methylpyridin-1-ium)) and (dipalmitoylphosphatidyl choline), respectively.[8]

antimicrobial nanocarriers are met by zwitterion-based platforms, but equally so by electrolyte-based ones.

The required transportation through the blood circulation is usually established by stealth-decoration of nano-antimicrobials or nanocarriers with poly(ethylene glycol) (PEG),[37] poly(ethylene oxide) (PEO),[38] poly(zwitterions)[17] or lipid-bound water[8] Clearance by the reticulo-endothelial system[39] is furthermore prevented by the use of nano-antimicrobials or antimicrobial nanocarriers with a diameter between around 5 to maximally 200 nm.

pH as a recognition sign to direct self-targeting platforms to an infection site works well in laboratory animals, living under controlled conditions and without co-morbidities. In humans however, the main problem to be solved with respect to self-targeting nano-antimicrobials and antimicrobial nanocarriers is the uniqueness of pH as a recognition sign for bacterial infection. An acid environment is not unique to a bacterial infection site and can also occur after prolonged exertion in

healthy tissue[40] or in malignant tumors.[41,42] Likely, unique environmental recognition signs in the human body for bacterial infection do not exist, warranting further research into zwitterions with dual-responsive functionalities for use in antimicrobial platforms. Possible additional internal recognitions signs could include temperature,[12] hypoxia,[9] presence of endogenous ROS[10] or enzymes,[43] either of bacterial[44] or endogenous origin.[7] Although temperature responsive zwitterions exist,[45–48] temperature on its own does not present a trigger that is unique for bacterial infection and in fact only bacterial enzymes would constitute a unique recognition sign. Pathogen-binding ligands can also be employed in self-targeting but are geared towards specific bacterial strains or species, unlike pH- or hypoxia-responsive approaches and may be chemically more difficult to establish.

However, (additional) triggers to direct antimicrobial platforms towards an infection site could also be external ones,

2320 | *J. Mater. Chem. B*, 2022, **10**, 2316–2322

This journal is © The Royal Society of Chemistry 2022

like UV or NIR irradiation or application of an applied magnetic field. Also here, zwitterion-based platforms might offer possibilities as light-responsive zwitterions have been described.[49–51] Precise light-assisted or magnetic-targeting to micrometer-sized infectious biofilms (estimated dimensions 4–200 μm[52]) and distribution of nano-antimicrobials over the entire depth of a biofilm is impossible with current clinical technologies that are better suited for external targeting of chemotherapeutic nanocarriers to centimeter-sized tumors.[53] As a general drawback, external triggering requires additional instrumentation and implies another hospital visit for a diseased patient.

Upon sensing an acidic pH, animal experiments have shown that pH is a sufficient recognition sign for property changes of zwitterion- or electrolyte-based antimicrobial platforms, yielding good penetration and accumulation in an infectious biofilm. Release of antimicrobial cargo inside an infectious biofilm is established as a sequential response under the influence of local pH conditions in a biofilm.[54]

In summary, self-targeting nano-antimicrobials and antimicrobial nanocarriers have provided a way to overcome the biofilm-barrier towards antimicrobial penetration and accumulation in an infectious biofilm. The combination of current antibiotics with various self-targeting platforms generating ROS inside an infectious biofilm or delivering antibiotics into the depth of a biofilm, has provided a new means to kill multi-drug resistant bacteria.[55,56] Therewith, a direly-needed pathway for future research has been lined out for the control of antimicrobial-resistant infections through the use of self-targeting nano-antimicrobials and nanocarriers, very similar to the pathway applied for the control of malignant tumors.[2,57] The next challenge with respect to bacterial infection control will be the translation of self-targeting nano-antimicrobials and antimicrobial nanocarriers from successful animal experiments to human clinical trials and application.

5. Conclusions

Self-targeting zwitterion-based nano-antimicrobials and antimicrobial nanocarriers have provided a way to overcome the biofilm-barrier towards antimicrobial penetration and accumulation in an infectious biofilm yielding efficient eradication of infectious biofilms. However, similar self-targeting can be established by electrolyte-based platforms. Up to what extent, full charge reversal and possibly shorter response times of zwitterion-based platforms constitute a clinical advantage above electrolyte-based platforms remains to be determined.

A second challenge towards further development of self-targeting platforms involves the design of molecules that respond to a unique internal recognition sign for infection or a combination of recognition signs. Zwitterions may also provide a good starting point for this, because light and temperature dependent zwitterions already exist. However, since temperature changes, alike pH changes, are not unique to infections, design of other responsive functionalities, preferably with an internal trigger, would be welcomed.

Author contributions

All the authors participated in the collection and analysis of the literature. D. Y. wang, L. Su, H. C. van der Mei, H. J. Busscher and L. Shi wrote and revised the manuscript.

Conflicts of interest

H. J. B. is also director of a consulting company SASA BV. The authors declare no potential conflicts of interest with respect to authorship and/or publication of this article. Opinions and assertions contained herein are those of the authors and are not construed as necessarily representing views of the funding organization or their respective employer(s).

Acknowledgements

References

1 K. Quan, J. Hou, Z. Zhang, Y. Ren, B. W. Peterson, H.-C. Flemming, C. Mayer, H. J. Busscher and H. C. van der Mei, *Crit. Rev. Microbiol.*, 2021, DOI: 10.1080/1040841x.2021.1962802.

2 Y. Liu, L. Shi, L. Su, H. C. van der Mei, P. C. Jutte, Y. Ren and H. J. Busscher, *Chem. Soc. Rev.*, 2019, **48**, 428–446.

3 O. S. Kluin, H. C. van der Mei, H. J. Busscher and D. Neut, *Expert Opin. Drug Delivery*, 2013, **10**, 341–351.

4 L. B. Norris, F. Kablaoui, M. K. Brilhart and P. B. Bookstaver, *Int. J. Antimicrob. Agents*, 2017, **50**, 308–317.

5 D. Neut, H. van de Belt, J. R. van Horn, H. C. van der Mei and H. J. Busscher, *Biomaterials*, 2003, **24**, 1829–1831.

6 C. Li, E. J. Cornel and J. Du, *ACS Appl. Polym. Mater.*, 2021, **3**, 2218–2232.

7 Y. Liu, H. J. Busscher, B. Zhao, Y. Li, Z. Zhang, H. C. van der Mei, Y. Ren and L. Shi, *ACS Nano*, 2016, **10**, 4779–4789.

8 D.-Y. Wang, G. Yang, H. C. van der Mei, Y. Ren, H. J. Busscher and L. Shi, *Angew. Chem., Int. Ed.*, 2021, **60**, 17714–17719.

9 W. Xiu, S. Gan, Q. Wen, Q. Qiu, S. Dai, H. Dong, Q. Li, L. Yuwen, L. Weng, Z. Teng, Y. Mou and L. Wang, *Research*, 2020, **2020**, 9426453.

10 S. Bertoni, Z. Liu, A. Correia, J. P. Martins, A. Rahikkala, F. Fontana, M. Kemell, D. Liu, B. Albertini, N. Passerini, W. Li and H. A. Santos, *Adv. Funct. Mater.*, 2018, **28**, 1806175.

11 Y. Gu and X. Han, *Int. J. Mol. Sci.*, 2020, **21**, 3329.

12 Y. Zhao, X. Dai, X. Wei, Y. Yu, X. Chen, X. Zhang and C. Li, *ACS Appl. Mater. Interfaces*, 2018, **10**, 14426–14437.

13 J. Tan, J. Tay, J. Hedrick and Y. Y. Yang, *Biomaterials*, 2020, **252**, 120078.

14 D. S. W. Benoit and H. Koo, *Nanomedicine*, 2016, **11**, 873–879.

15 A. Gupta, R. Das, G. Yesilbag Tonga, T. Mizuhara and V. M. Rotello, *ACS Nano*, 2018, **12**, 89–94.

This journal is © The Royal Society of Chemistry 2022

J. Mater. Chem. B, 2022, **10**, 2316–2322 | **2321**

16 Y. Ding, J. Liu, X. Li, L. Xu, C. Li, L. Ma, J. Liu, R. Ma, Y. An, F. Huang, Y. Liu and L. Shi, *Mater. Chem. Front.*, 2019, **3**, 1159–1167.

17 S. Tian, L. Su, Y. Liu, J. Cao, G. Yang, Y. Ren, F. Huang, J. Liu, Y. An, H. C. van der Mei, H. J. Busscher and L. Shi, *Sci. Adv.*, 2020, **6**, eabb1112.

18 S. Wang, F. Zhang, G. Yu, Z. Wang, O. Jacobson, Y. Ma, R. Tian, H. Deng, W. Yang, Z.-Y. Chen and X. Chen, *Theranostics*, 2020, **10**, 6629–6637.

19 A.-H. Ranneh, H. Takemoto, S. Sakuma, A. Awaad, T. Nomoto, Y. Mochida, M. Matsui, K. Tomoda, M. Naito and N. Nishiyama, *Angew. Chem., Int. Ed.*, 2018, **57**, 5057–5061.

20 C. L. Walsh, J. Nguyen and F. C. Szoka, *Chem. Commun.*, 2012, **48**, 5575–5577.

21 Y. Wang, D. Huang, X. Wang, F. Yang, H. Shen and D. Wu, *Biomater. Sci.*, 2019, **7**, 3238–3248.

22 L. D. Blackman, P. A. Gunatillake, P. Cass and K. E. S. Locock, *Chem. Soc. Rev.*, 2019, **48**, 757.

23 T. Ramasamy, B. K. Poudal, H. Ruttala, J. Y. Choi, T. D. Hieu, K. Umadevi, Y. S. Youn, H. G. Choi, C. S. Yong and J. O. Kim, *Colloids Surf., B*, 2016, **146**, 152–160.

24 M. C. Smith, R. M. Crist, J. D. Clogston and S. E. McNeil, *Anal. Bioanal. Chem.*, 2017, **409**, 5779–5787.

25 C.-Y. Sun, Y. Liu, J.-Z. Du, Z.-T. Cao, C.-F. Xu and J. Wang, *Angew. Chem., Int. Ed.*, 2016, **55**, 1010–1014.

26 P. Li, S. Liu, G. Zhang, X. Yang, W. Cao, X. Gong and X. Xing, *ACS Appl. Bio Mater.*, 2020, **3**, 1105–1115.

27 R. Guo, K. Li, B. Tian, C. Wang, X. Chen, X. Jiang, H. He and W. Hong, *J. Nanobiotechnol.*, 2021, **19**, 232.

28 L. Ritsma, E. J. A. Steller, S. I. J. Ellenbroek, O. Kranenburg, I. H. M. Borel Rinkes and J. van Rheenen, *Nat. Protoc.*, 2013, **8**, 583–594.

29 A. Erfani, J. Seaberg, C. P. Aichele and J. D. Ramsey, *Biomacromolecules*, 2020, **21**, 2557–2573.

30 H. Wu, C.-J. Lee, H. Wang, Y. Hu, M. Young, Y. Han, F.-J. Xu, H. Cong and G. Cheng, *Chem. Sci.*, 2018, **9**, 2540–2546.

31 Y. Chang, S.-C. Liao, A. Higuchi, R.-C. Ruaan, C.-W. Chu and W.-Y. Chen, *Langmuir*, 2008, **24**, 5453–5458.

32 R. Safavi-Sohi and A. Ghassempour, *Nanomed. Res. J.*, 2018, **3**, 89–95.

33 S. Peng, B. Ouyang, Y. Men, Y. Du, Y. Cao, R. Xie, Z. Pang, S. Shen and W. Yang, *Biomaterials*, 2020, **231**, 119680.

34 J. Zhang, L. Liu, L. Wang, W. Zhu and H. Wang, *J. Mater. Chem. B*, 2020, **8**, 8908–8913.

35 W. Yang, S. Liu, T. Bai, A. J. Keefe, L. Zhang, J.-R. Ella-Menye, Y. Li and S. Jiang, *Nano Today*, 2014, **9**, 10–16.

36 H. Ou, T. Cheng, Y. Zhang, J. Liu, Y. Ding, J. Zhen, W. Shen, Y. Xu, W. Yang, P. Niu, J. Liu, Y. An, Y. Liu and L. Shi, *Acta Biomater.*, 2018, **65**, 339–348.

37 V. M. Ragaseema, S. Unnikrishnan, V. Kalliyana Krishnan and L. K. Krishnan, *Biomaterials*, 2012, **33**, 3083–3092.

38 Y. Xi, Y. Wang, J. Gao, Y. Xiao and J. Du, *ACS Nano*, 2019, **13**, 13645–13657.

39 E. Blanco, H. Shen and M. Ferrari, *Nat. Biotechnol.*, 2015, **33**, 941–951.

40 A. Cordova, F. J. Navas and J. F. Escanero, *Biol. Trace Elem. Res.*, 1993, **39**, 13–20.

41 X. Zhang, Y. Lin and R. J. Gillies, *J. Nucl. Med.*, 2010, **51**, 1167–1170.

42 A. Zhang, L. Yao and M. An, *Chem. Commun.*, 2017, **53**, 12826–12829.

43 Y. N. Albayaty, N. Thomas, M. Jambhrunkar, M. Al-Hawwas, A. Kral, C. R. Thorn and C. A. Prestidge, *Int. J. Pharm.*, 2019, **566**, 329–341.

44 D. Pornpattananangkul, L. Zhang, S. Olson, S. Aryal, M. Obonyo, K. Vecchio, C.-M. Huang and L. Zhang, *J. Am. Chem. Soc.*, 2011, **133**, 4132–4139.

45 W. Fu, C. Luo, E. A. Morin, W. He, Z. Li and B. Zhao, *ACS Macro Lett.*, 2017, **6**, 127–133.

46 H. Sun, J. Chen, X. Han and H. Liu, *Mater. Sci. Eng., C*, 2018, **82**, 284–290.

47 C.-Y. Chen and H.-L. Wang, *Macromol. Rapid Commun.*, 2014, **35**, 1534–1540.

48 C. M. E. Tan, G. V. Dizon, S.-H. Chen, A. Venault, Y.-N. Chou, L. Tayo and Y. Chang, *J. Mater. Chem. B*, 2020, **8**, 8853–8863.

49 Y. Zhou, R. Chen, H. Yang, C. Bao, J. Fan, C. Wang, Q. Lin and L. Zhu, *J. Mater. Chem. B*, 2020, **8**, 727–735.

50 X. Zhang, M. Zhang, M. Wu, L. Yang, R. Liu, R. Zhang, T. Zhao, C. Song, G. Liu and Q. Zhu, *Polymers*, 2021, **13**, 2392.

51 A. Balamurugan and H.-i. Lee, *Macromolecules*, 2016, **49**, 2568–2574.

52 T. Bjarnsholt, M. Alhede, M. Alhede, S. R. Eickhardt-Soerensen, C. Moser, M. Kuhl, P. O. Jensen and N. Høiby, *Trends Microbiol.*, 2013, **21**, 466–474.

53 K. Quan, Z. Zhang, Y. Ren, H. J. Busscher, M. H. C. van der Mei and B. W. Peterson, *J. Mater. Sci. Technol.*, 2021, **69**, 69–78.

54 H. Koo, R. N. Allan, R. P. Howlin, P. Stoodley and L. Hall-Stoodley, Targeting microbial biofilms: current and prospective therapeutic strategies, *Nat. Rev. Microbiol.*, 2017, **15**, 740–755.

55 H. Chen, J. Yang, L. Sun, H. Zhang, Y. Guo, J. Qu, W. Jiang, W. Chen, J. Ji, Y.-W. Yang and B. Wang, *Small*, 2019, **15**, 1903880.

56 D. Hassan, C. A. Omolo, V. O. Fasiku, A. A. Elrashedy, C. Mocktar, M. E. S. Soliman, T. Govender, C. A. Omolo and B. Nkambule, *Pharmaceutics*, 2020, **12**, 2–30.

57 M. Zhang, X. Chen, C. Li and X. Shen, *J. Controlled Release*, 2020, **319**, 46–62.

2322 | *J. Mater. Chem. B*, 2022, **10**, 2316–2322

This journal is © The Royal Society of Chemistry 2022